Pseudopotentials for correlated-electron calculations

Y. Lee, P. R. C. Kent,* M. D. Towler, R. J. Needs, and G. Rajagopal
Cavendish Laboratory, University of Cambridge, Madingley Road, Cambridge CB3 0HE, United Kingdom
(Received 10 May 2000; revised manuscript received 31 July 2000)

We describe a semiempirical method for constructing pseudopotentials for use in correlated wave-function calculations which involves using a combination of calculated and experimental quantities. The pseudopotentials are generated from single-valence-electron configurations and satisfy a norm-conservation condition. Core relaxation and core-polarization effects are taken into account. Detailed results for a typical atom with *s* and *p* valence electrons (silicon) and a transition metal atom (titanium) are given. The method works very well for silicon but is not satisfactory for titanium.

I. INTRODUCTION

Pseudopotentials or effective core potentials are commonly used in electronic structure calculations to remove the inert core electrons from the problem and to improve the computational efficiency. In this paper we study the performance of pseudopotentials in correlated wave-function approaches. Our particular interest is in the diffusion quantum Monte Carlo (DMC) method.[1,2] This is a very accurate technique which is promising for applications to large systems because the computational effort scales as the third power of the number of electrons, which is very favorable compared with other correlated wave-function approaches. Despite this favorable scaling with the number of atoms the scaling with the atomic number Z of the atoms is approximately $Z^{5.5-6.5}$, which effectively rules out applications to heavy atoms.[3,2] The use of a pseudopotential serves to reduce the effective value of Z, and although errors are inevitably introduced, the gain in computational efficiency is sufficient to make applications to heavy atoms feasible. Although our study has been performed with the DMC method in mind, the conclusions are relevant to other correlated wave-function methods.

Accurate pseudopotentials for single-particle theories such as Kohn-Sham density functional theory (KS-DFT) and Hartree-Fock (HF) theory are well developed, but pseudopotentials for correlated wave-function calculations present additional challenges. HF-based pseudopotentials[4] give quite good results within correlated wave-function calculations for many atoms. The reason is presumably that for many atoms core-core and core-valence correlations have only a small influence on the valence electrons. Within single-particle theories such as KS-DFT and HF theory modern pseudopotentials often give very accurate results. The transferability of these pseudopotentials is significantly improved by imposing the ''norm-conservation''[5,6,4] condition, which ensures that for the reference configuration they reproduce the exact orbitals (including the normalization) outside of the core radius. The importance of the norm-conservation condition is that it ensures that the linear variation of the scattering properties of the core with the energy of an incident valence electron is correctly reproduced. For many atoms norm-conserving pseudopotentials generated within KS-DFT and HF theory are quite similar, so the precise treatment of the electron-electron interaction does not appear to be critical. In addition, some of the effects of core-valence correlation may be included in pseudopotential correlated wave-function calculations by adding ''core-polarization potentials'' (CPP's).[7] The basic idea is that the core electrons respond very rapidly to changes in the positions of the valence electrons and the effect can be approximately described by a polarization of the core arising from the instantaneous electric field of the valence electrons.

There is, however, a need for more accurate pseudopotentials for use in correlated wave-function calculations. The pseudopotentials currently used in correlated calculations perform significantly worse than, for example, KS-DFT pseudopotentials in a KS-DFT calculation. Given that the idea of using correlated methods is to obtain higher accuracy than in KS-DFT or HF calculations, this is a significant shortcoming. In this paper we describe a semi-empirical procedure for obtaining pseudopotentials for correlated calculations. We use a combination of calculated quantities and the experimental ionization energies for a single electron in the field of an isolated ion. These energies could be calculated, which would yield a scheme free from experimental input, but we believe that using the experimental energies leads to improved accuracy. Our procedure is similar in some respects to the empirical procedures used in the 1960s,[8,9] in which pseudopotentials were generated for an electron in the field of an ion using experimental energies. However, our procedure differs from these earlier versions in four important ways: (i) our pseudopotentials obey a norm-conservation condition, (ii) we improve the description of core-valence correlation effects by including core-polarization effects in a consistent manner, (iii) we include corrections for the core relaxation effects arising from generating the pseudopotential in ionized configurations, and (iv) we include an accurate representation of the Hartree and exchange potentials outside of the core. The method is illustrated with detailed results for the silicon and titanium atoms, and the accuracy of our semi-empirical pseudopotential is compared with a number of other potentials.

II. PSEUDOPOTENTIALS FROM SINGLE-VALENCE-ELECTRON CONFIGURATIONS

Acioli and Ceperley[10] showed using perturbation theory that the quality of a many-body pseudopotential depends on

an accurate description of the one-body, two-body, etc., density matrices outside the core region. The most important quantity is the one-body density matrix, whose eigenfunctions are the natural orbitals. It is therefore important to ensure that the natural orbitals of the pseudoatom are correct outside of the core region. For single valence electrons this theory reduces to the standard concept of norm conservation.

Our semiempirical pseudopotentials are constructed from single-valence-electron configurations; e.g., for Si we use the $[\mathrm{Ne}]3s^1$, $[\mathrm{Ne}]3p^1$, and $[\mathrm{Ne}]3d^1$ configurations. The minimum requirements that a norm-conserving pseudopotential for angular momentum l must satisfy are that it reproduce correctly the following quantities in the reference configuration: (i) the potential felt by the valence electron outside of some core radius, r_c^l, (ii) the total amount of valence electronic charge outside of r_c^l, and (iii) the energy eigenvalue ϵ_l. In the next sections we explain how each of these three quantities is calculated.

A. Hartree-Fock potential

Consider a single valence electron in the field of an isolated ion. Within HF theory the potential felt by the electron is the sum of the interaction with the nucleus of charge Z and the Hartree and exchange interactions with the core,

$$\hat{V}_{\mathrm{HF}} = -\frac{Z}{r} + \hat{V}^{\mathrm{H}} + \hat{V}^{\mathrm{X}}. \tag{1}$$

The HF potential accounts for most of the effects felt by the valence electron, but neglects correlation effects.

B. Core-polarization potential

If the core-valence correlation is weak, it is reasonable to write the effective potential felt by the valence electrons as the sum of the HF potential and a correlation potential, $\hat{V}^{\mathrm{C}}$. An approximate correlation potential can be obtained within the framework of core polarization potentials. Callaway[11] developed a theory for $\hat{V}^{\mathrm{C}}$ which involves an adiabatic separation between the core and valence electrons, in which the core electrons move instantaneously in response to the motion of the valence electrons. Callaway showed that, after a series of approximations, $\hat{V}^{\mathrm{C}}$ could be approximated by a dipole term which represents the polarization of the core due to the electric field of the valence electrons (and other ions, if present). This leads to the CPP approximation[7] for $\hat{V}^{\mathrm{C}}$,

$$\hat{V}_{\mathrm{CPP}} = -\frac{1}{2}\alpha_c \mathbf{E}_c \cdot \mathbf{E}_c, \tag{2}$$

where α_c is the static polarizability of the core and $\mathbf{E}_c$ is the effective electric field acting on the core due to the valence electrons. When a valence electron is within the core this equation overestimates the core polarization, which must be zero when the electron is at the nucleus. To make the CPP vanish at the origin Müller *et al.*[7] cut off $\mathbf{E}_c$ as

$$\mathbf{E}_c = \sum_i \frac{\mathbf{r}_i}{r_i^3} f\left(\frac{r_i}{\bar{r}}\right), \tag{3}$$

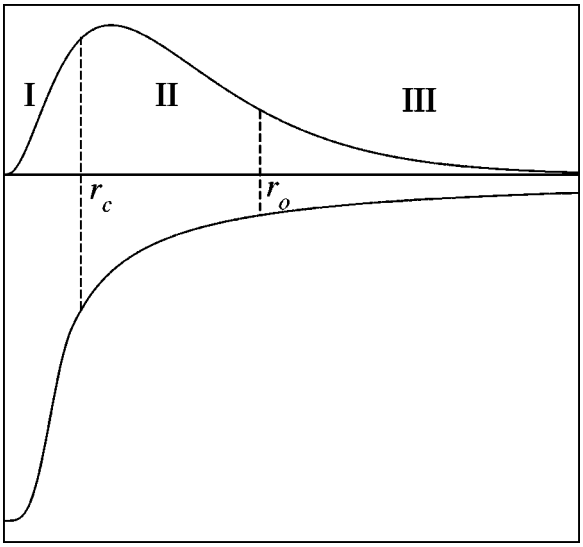

FIG. 1. The division of space into the core region (I), $0<r<r_c^l$, the intermediate region (II), $r_c^l<r<r_o$, and the outer region (III), $r>r_o$, for the s valence state of Si. The upper curve shows the pseudo-orbital while the lower curve shows the pseudopotential.

where $\mathbf{r}_i$ is the position of the ith valence electron, and $\bar{r}$ is an adjustable parameter. Müller *et al.*[7] investigated several forms of the cutoff function $f(x)$, and we use one of their forms,

$$f(x) = (1 - e^{-x^2})^2, \tag{4}$$

which was also used by Shirley and Martin.[12] Inserting Eq. (3) into Eq. (2) yields

$$\begin{aligned}\hat{V}_{\mathrm{CPP}} &= -\frac{\alpha_c}{2}\sum_i \frac{1}{r_i^4} f^2\left(\frac{r_i}{\bar{r}}\right) - \frac{\alpha_c}{2}\sum_{i\neq j}\frac{\mathbf{r}_i\cdot\mathbf{r}_j}{r_i^3 r_j^3} f\left(\frac{r_i}{\bar{r}}\right) f\left(\frac{r_j}{\bar{r}}\right) \\ &= V^e_{\mathrm{CPP}} + V^{e\text{-}e}_{\mathrm{CPP}},\end{aligned} \tag{5}$$

which is a sum of one- and two-electron terms. The valence electrons prefer to sit on either side of the core so as to minimize the interaction energy, but the introduction of the two-electron term $V^{e\text{-}e}_{\mathrm{CPP}}$ opposes this because it penalizes configurations in which $\mathbf{r}_i\cdot\mathbf{r}_j<0$. The expectation values of V^e_{CPP} and $V^{e\text{-}e}_{\mathrm{CPP}}$ therefore tend to cancel one another.

C. Valence potential in different regions

In order to construct our semiempirical pseudopotential we divide the radial space into three regions as illustrated in Fig. 1. The core radius of a pseudopotential for a particular angular momentum, r_c^l, is conventionally chosen between the outermost node and extremum of the all-electron valence orbital, and the values that we have used for Si and Ti are given in Table I. Region I ($0<r<r_c^l$) is the core region for angular momentum l. We do not have to specify the potential in region I explicitly as it will be fixed by inversion of the (pseudo) Schrödinger equation. In the intermediate region II ($r_c^l<r<r_o$) the single-valence electron experiences the HF potential from the core and the correlation potential. We

TABLE I. Core radii, r_c^l, and the radius defining the outer region r_o in au for Si and Ti.

Atom	r_c^0	r_c^1	r_c^2	r_o
Si	1.75	1.8	2.0	20.17
Ti	2.3	2.6	1.0	30.46

write the orbital as the product of radial and angular parts, $\Phi_{lm}(\mathbf{r})=[\phi_l(r)/r]Y_{lm}(\theta,\phi)$, and the equation for ϕ_l in region II becomes

$$\left(-\frac{1}{2}\frac{d^2}{dr^2}+\frac{l(l+1)}{2r^2}-\frac{Z}{r}+V_{\rm II}^{\rm H}+V_{\rm II}^{\rm X}+V_{\rm II}^{\rm C}\right)\varphi_l^{\rm II}(r)=\epsilon_l\varphi_l^{\rm II}(r), \tag{6}$$

where ϵ_l is the eigenvalue and

$$V_{\rm II}^{\rm H}(r)=\sum_c\,(4l_c+2)\int_0^\infty\frac{1}{r_>}\varphi_{l_c}(r')\varphi_{l_c}(r')dr',$$

$$V_{\rm II}^{\rm X}(r)=-\sum_{c,k}\,(2l_c+1)\begin{pmatrix}l & k & l_c\\ 0 & 0 & 0\end{pmatrix}^2\frac{\varphi_{l_c}(r)}{\varphi_l(r)}\times\int_0^\infty\frac{r_<^k}{r_>^{k+1}}\varphi_{l_c}(r')\varphi_l(r')dr',$$

$$V_{\rm II}^{\rm C}(r)=-\frac{\alpha_c}{2}\frac{1}{r^4}f^2\left(\frac{r}{=}{r}\right), \tag{7}$$

where the $\varphi_l(r)$ represents all-electron restricted HF radial orbitals for the singly valent configurations, $r_<(r_>)$ is the lesser (greater) of r and r', and

$$\begin{pmatrix}l & k & l_c\\ 0 & 0 & 0\end{pmatrix}$$

is a $3j$ symbol. The summations are over the core states, which are denoted by c. Here k is an integer $\geqslant 0$, and $V_{\rm II}^{\rm X}(r)$ is nonzero for $|l_c-l|\leqslant k\leqslant l_c+l$ with $(k+l_c+l)$ even. Note that the self-interaction of the single valence electron is omitted from Eq. (7).

For some atoms, e.g., Si, we find that for realistic core radii (see Table I) $V_{\rm II}^{\rm H}$, $V_{\rm II}^{\rm X}$, and $V_{\rm II}^{\rm C}$ are already very close to their asymptotic values in region II, i.e.,

$$V_{\rm II}^{\rm H}(r)=\frac{N_c}{r},$$

$$V_{\rm II}^{\rm X}(r)=0,$$

$$V_{\rm II}^{\rm C}(r)=-\frac{\alpha_c}{2r^4}, \tag{8}$$

where N_c is the number of core electrons. In general we have found that the asymptotic forms of Eq. (8) are accurate to about 10^{-3} eV provided that r_c^l is chosen so that at least 99% of the total core charge is confined to region I. This criterion allows reasonable core radii for atoms with s and p valence electrons, but not for transition metal atoms, for which the full forms of Eq. (7) must be used.

The outer radius r_o is chosen to be large enough so that in region III ($r>r_o$) the correlation potential is negligible and the Hartree and exchange potentials from the core dominate so that we have

$$\left(-\frac{1}{2}\frac{d^2}{dr^2}+\frac{l(l+1)}{2r^2}-\frac{Z-N_c}{r}\right)\phi_l^{\rm III}(r)=\epsilon_l\phi_l^{\rm III}(r). \tag{9}$$

We have chosen r_o such that $V_{\rm CPP}^e(r\geqslant r_o)\leqslant 10^{-6}$ Ry (see Table I).

D. Valence eigenvalues

For the valence eigenvalues we use the experimental values for the energy differences between the singly-valent ions and the bare core, i.e., the ionization energy. These energies were obtained from the compilation of Bashkin and Stoner[13] by taking degeneracy-weighted averages of the spin-orbit-split levels. The advantage of using the experimental energies is that they contain both relativistic and correlation effects, which are difficult to include in accurate many-body calculations. Of course we could obtain these energies from calculations, which would remove the need for any experimental input in our scheme. However, for large Z atoms it would certainly be difficult to calculate highly accurate energies and therefore we prefer to use the experimental ones.

Using the experimental ionization energies ϵ_l guarantees that we obtain the correct asymptotic form of the charge density for the singly-valent configuration,

$$\rho_l(r)\propto\exp[-2(2|\epsilon_l|)^{1/2}r]. \tag{10}$$

Within HF theory the asymptotic form of the HF charge density is given by a similar expression, but with the ionization energy replaced by the HF eigenvalue of the highest occupied state, which is not in general equal to the HF ionization energy. In our scheme we would like to reproduce the correct asymptotic form of the charge density and therefore we follow Eq. (10) and use the experimental ionization energy. In Sec. II F we will equate changes in the HF valence eigenvalues to changes in the ionization energy arising from core relaxation. This procedure is justified because we are creating pseudopotentials using single-valent configurations, for which the change in the eigenvalue is equal to the change in the ionization energy.

E. Norms of the valence wave functions

In single-particle theories there is no ambiguity concerning the definition of core and valence charge densities, which is simply a matter of labeling the orbitals as belonging to the core or valence, but in a correlated many-electron theory one cannot make a wholly unambiguous definition of the core and valence charge densities. However, physically, the core charge density must be contained within some reasonably small radius, which can easily be estimated from single-particle calculations. We can assert that even in a many-body calculation all charge outside of this radius must be valence charge.

By fixing the valence eigenvalue and the potential for $r\geqslant r_c^l$ we have fixed the functional form of the valence orbital for $r\geqslant r_c^l$, but not its normalization. To find the normaliza-

tion we must know the amount of valence charge ρ_l^v outside of some radius $r_n \geq r_c^l$. We obtain this charge density from all-electron calculations for the single-valent ions. We have used a variety of methods to calculate ρ_l^v, including the local spin-density approximation (LSDA) to KS-DFT, HF theory and configuration interaction with single and double excitations (CISD). For the LSDA calculations we used an atomic code based on a finely spaced radial grid, while for the HF calculations we used the code of Fröse Fischer,[14] which also uses a radial grid. The CISD calculations were performed using the GAUSSIAN 94 code.[15] The CISD calculations give excellent correlation energies, but the GAUSSIAN basis set gives a poor description of the charge density far from the atom. Choosing r_n too large would therefore lead to an inaccurate value of the norm, and in our calculations we have chosen $r_n = r_c^l$. This choice is not always large enough to ensure that the core charge density is confined within r_n, but in these cases we correct the norm using the results of LSDA or HF calculations. In practice these different methods give norms in very close agreement with one another, and the norm appears to be insensitive to the description of the electron correlation.

F. Core relaxation

Core relaxation in an isolated atom refers to the change in the distribution of the core electrons which occurs when the configuration of the valence electrons is altered. We generate pseudopotentials from a particular reference configuration of the atom, which therefore includes the effect of the core frozen in this configuration. The semiempirical pseudopotentials are generated in highly ionized configurations although we would normally like to use them in near neutral configurations. Clearly errors will be introduced if the relaxation of the core on going from the ionized to the neutral configuration is significant. The idea of our core relaxation correction procedure is as follows. Core relaxation changes the pseudopotential and hence alters the valence eigenvalue and the amount of valence charge outside of r_c^l. However, the changes in the pseudopotential will be mainly confined to the core region and therefore we can retain the potentials of Eqs. (6) and (9) in regions II and III while applying corrections to the valence eigenvalue and norm. Our correction procedure is therefore to generate the pseudopotential without changing the potential outside the core region, but adding small corrections to the norms of the valence orbitals and their eigenvalues.

Although the idea of core relaxation corrections is natural enough, it turns out that they are difficult to define mathematically. We have used the following definition which is meaningful within independent electron theories such as HF and KS-DFT. Suppose we construct the $3d$ pseudopotential for Ti within our semiempirical scheme which uses single-valence-electron configurations. What is the change in the ϵ_{3d} eigenvalue due to using the core of the ionized atom rather than the core of the neutral atomic ground state? The HF equations for the ionized configuration are

$$\left(-\frac{1}{2}\frac{d^2}{dr^2} + \frac{l(l+1)}{2r^2} - \frac{Z}{r} + V^{\mathrm{H}}[\phi_c^i, \phi_{3d}^i] + V^{\mathrm{X}}[\phi_c^i, \phi_{3d}^i] \right) \phi_{nl}^i = \epsilon_{nl}^i \phi_{nl}^i , \tag{11}$$

TABLE II. The experimental ionization energies ϵ_l, the core relaxation energies $\Delta\epsilon_l$, and the change in the norm due to core relaxation, ΔN, for Si and Ti.

Orbital	ϵ_l (Ry)	$\Delta\epsilon_l$ (Ry)	ΔN
Si $3s$	−3.317903	−0.00413	0.00140
Si $3p$	−2.665468	−0.00415	0.00204
Si $3d$	−1.856442	−0.00246	0.00215
Ti $4s$	−2.447521	−0.0595	0.0289
Ti $4p$	−2.009403	−0.0571	0.0369
Ti $3d$	−3.177990	−0.1313	0.0174

where V^{H} and V^{X} are the Hartree and exchange potentials, ϕ_c^i and ϕ_{3d}^i are the core orbitals and the valence orbital, and i denotes the ionized configuration. We now perform a second calculation with the core orbitals in V^{H} and V^{X} replaced by those obtained from a calculation in the neutral atomic ground state, ϕ_c^0. These HF equations are then solved with the ϕ_c^0 orbitals fixed to give the energies ϵ_{nl}^0 and associated orbitals ϕ_{nl}^0. The change in the $3d$ eigenvalue due to the core relaxation is then

$$\Delta\epsilon_d = \epsilon_{3d}^0 - \epsilon_{3d}^i , \tag{12}$$

and the change in the amount of charge in the core region is

$$\Delta N_d = \int_0^{r_c^{l=2}} (|\phi_{3d}^0|^2 - |\phi_{3d}^i|^2)\, dr . \tag{13}$$

The values of $\Delta\epsilon$ and ΔN for Si and Ti are given in Table II. Clearly one can make an analogous definition within KS-DFT theory which we have found gives similar results. We have calculated the $\Delta\epsilon$ of Eq. (12) and the ΔN of Eq. (13) for the s, p, and d channels of all atoms up to Zn. The $\Delta\epsilon$ increases in magnitude across the rows and down the columns of the periodic table. The ΔN shows similar trends, although for many atoms they are small. We find that $\Delta\epsilon$ is almost always negative while ΔN is almost always positive. The reason for this is that the core of the ionized atom is more compact so that the nuclear charge is more effectively screened and consequently the potential felt by the valence electrons is less attractive.

III. CONSTRUCTION OF THE PSEUDOPOTENTIALS

The required solution of the Schrödinger equation in region III [Eq. (9)] is

$$\phi_l^{\mathrm{III}}(r) \propto W_{x,l+1/2}\left(\frac{2(Z-N_c)}{x} r \right), \tag{14}$$

where $W_{x,y}(z) = e^{-z/2} z^{y+1/2} U(y-x+1/2, 2y+1; z)$ is the Whittaker function of the second kind, U is the confluent hypergeometric function of the second kind,[16] and $x = (Z - N_c)/\sqrt{2|\epsilon_l|}$. The asymptotic form of this expression yields Eq. (10), as required.

The Whittaker function gives the form of the solution throughout region III. We proceed by choosing a value for $\phi_l^{\mathrm{III}}(r_o)$. The corresponding radial derivative of $\phi_l^{\mathrm{III}}(r_o)$ is then fixed from Eq. (14). Using the desired value of the

valence eigenvalue we then integrate Eq. (6) inwards from r_o to $r=r_c^l$, numerically. At this point we evaluate the norm of ϕ_l over regions II and III and then renormalize ϕ_l to the desired value.

So far we have fixed the pseudo-orbital in regions II and III. We now proceed to calculate the pseudo-orbital inside r_c^l and invert the Schrödinger equation to obtain the corresponding pseudopotential. For this purpose we use the standard Troullier-Martins (TM) scheme[17] which was developed for generating pseudopotentials within KS-DFT. Within this scheme the pseudo-orbital in the core region is given by

$$\phi_l^I(r)=r^{l+1}\exp\left[\sum_{k=0}^{6} c_{2k}r^{2k}\right], \tag{15}$$

where the c_i are coefficients to be determined. In the TM scheme seven conditions are used to determine the seven coefficients: continuity of the pseudo-orbital and its first four derivatives at the core radius, zero curvature of the pseudopotential at the origin, and the norm-conservation condition. Troullier and Martins investigated a number of variants of this scheme and found that this one gave smooth and transferable pseudopotentials. Note that the exponent in Eq. (15) contains only even powers. The absence of the odd powers in the exponential of Eq. (15) ensures that all the odd derivatives of the screened pseudopotential are zero at the origin, which helps to keep the pseudopotential smooth. The absence of the term linear in r forces the pseudopotential to be finite at the origin. This allows the use of larger time steps in DMC calculations,[18] and it could also be advantageous in other correlated wave-function methods.

Once $\phi_l^{\mathrm{I}}(r)$ is determined, the pseudopotential $V_l(r)$ is obtained in region I by inverting the radial Schrödinger equation,

$$V_l(r)=\epsilon_l-\frac{l(l+1)}{2r^2}+\frac{1}{2\phi_l^{\mathrm{I}}}\frac{d^2\phi_l^{\mathrm{I}}}{dr^2}. \tag{16}$$

This completes the construction of the semiempirical pseudopotential.

When testing the effects of core polarization we have used the CPP defined by Eqs. (2)–(5), with the parameters of Shirley and Martin.[12] Shirley and Martin calculated core-polarizabilities α_c and parameters $\bar{r}$ for 32 elements. The $\bar{r}$ parameters were obtained by forcing the expectation values of the CPP and of their calculated generalized GW self-energy to be equal for the lowest valence states in bare ion configurations. They give CPP's for use with relativistic HF (i.e., Dirac-Fock) pseudopotentials [Table 1(a) of Ref. 12] and nonrelativistic ones [Table 1(b) of Ref. 12]. We use the parameters of Table 1(b) for our HF pseudopotentials but those of Table 1(a) for our semiempirical pseudopotentials because these incorporate the experimental valence eigenvalues which contain relativistic effects. The differences between using the relativistic and nonrelativistic parameters is small for the atoms we have considered. Note that our semiempirical pseudopotential includes the one-electron CPP term V_{CPP}^{e}, and therefore to form a consistent CPP potential we add only the $V_{\mathrm{CPP}}^{e\text{-}e}$ term from Table 1(a) of Ref. 12.

We have also generated pseudopotentials within LSDA and HF theory using the same core radii and the TM scheme. These pseudopotentials were generated in the neutral ground state. HF pseudopotentials created by such a scheme have a long-range tail due to the exchange interaction, which we have cut off, as others have done before.[19,12] We have also tested the Hay-Wadt pseudopotentials for Si (Ref. 20) and Ti (Ref. 21), and the Hay-Wadt (HW) small core[22] pseudopotential for Ti, in which the $3s$ and $3p$ electrons are included in the valence. For Ti we also tested the Dirac-Fock (DF) pseudopotential of Hurley *et al.*[23]

IV. TESTING THE PSEUDOPOTENTIALS

We have tested all of our pseudopotentials by performing atomic calculations using the fixed-node DMC method. Some of the tests have been repeated with the configuration-interaction method with single and double excitations (CISD) using the GAUSSIAN94 package,[15] which gave very similar results. For the single-valence-electron states we also calculate the energies by numerical integration on a grid, which yields essentially exact results.

In DMC (Refs. 1 and 2) imaginary time evolution of the Schrödinger equation is used to evolve an ensemble of $3N$-dimensional electronic configurations towards the ground state. Importance sampling is incorporated via a guiding wave function Φ_T. We use the fixed-node approximation, in which the nodal surface of the wave function is constrained to equal that of Φ_T. The fixed-node DMC method generates the distribution $\Phi_T\Psi$, where Ψ is the best (lowest energy) wave function with the same nodes as Φ_T. Our guiding wave functions are of the Slater-Jastrow type:

$$\Phi_T=\sum_n \alpha_n D_n^{\uparrow}D_n^{\downarrow}\exp\left[-\sum_{i<j}^{N} u_{\sigma_i,\sigma_j}(r_{ij},r_i,r_j)\right], \tag{17}$$

where there are N electrons in the system, u is a two-electron correlation factor which depends on the relative spins of the electrons σ_i and σ_j, r_{ij} is the separation of the electrons, and r_i and r_j are their distances from the nucleus. $D_n^{\uparrow}$ and $D_n^{\downarrow}$ are Slater determinants of up- and down-spin single-particle orbitals which were obtained from LSDA calculations for the electronic configurations of interest. Some calculations were repeated using HF orbitals, but they gave almost identical results. The u function was expanded as a polynomial in r_{ij}, r_i, and r_j which was constrained to obey the electron-electron cusp conditions.[24] For Si we included only powers of r_{ij} and r_i, giving a total of 24 parameters, but for Ti we added terms in $r_i^{\alpha}r_j^{\beta}$, $r_i^{\alpha}r_{ij}^{\beta}$, and $r_i^{\alpha}r_j^{\beta}r_{ij}^{\gamma}$ (α,β,γ integer), giving a total of 34 parameters. The optimal parameter values were obtained by minimizing the variance of the energy.[25,26] The nonlocal component of the electron-ion energy was evaluated using the ''locality approximation.''[27] The error in making this approximation is of order $(\Phi_T-\Psi)^2$, so that it is important that the trial wave function be accurate.

The DMC method can also be used to study excited states. It is straightforward to show that if the nodal surface of the guiding wave function is equal to that of an exact eigenstate, then the fixed-node DMC algorithm gives the exact energy of that eigenstate (apart from the locality approxi-

TABLE III. Acronyms for the different pseudopotentials and a measure of the error in the pseudopotentials, Δ.

Acronym	Pseudopotential	Δ Si	Δ Ti
HWL	Hay-Wadt large core, Refs. 20,21	0.139	0.671
HWS	Hay-Wadt small core, Ref. 22		0.185
DF	Dirac-Fock, Ref. 23		0.379
HF	Hartree-Fock	0.052	0.056
HF+CPP	Hartree-Fock with CPP	0.015	0.426
LSDA	Relativistic LSDA	0.075	0.929
SE	Semiempirical	0.022	0.865
SE+$V_{\mathrm{CPP}}^{e\text{-}e}$	Semiempirical with e-e CPP	0.019	1.006
SE-relax+$V_{\mathrm{CPP}}^{e\text{-}e}$	Semiempirical with relaxation and e-e CPP	0.010	0.803

mation). Recently, the existence of variational theorems within the fixed-node DMC method have been analyzed by Foulkes, Hood, and Needs.[28]

For each Si pseudopotential we have calculated the energies of nine atomic configurations using the DMC method, while for each Ti pseudopotential we have calculated the energies of ten atomic configurations. For most states only a single determinant is required to produce a guiding wave function with the correct quantum numbers, but for the $3s^1 3p^1(^1P)$ state of Si and the $3d^1 4s^1(^1D)$ state of Ti two determinants are required. For the (^3F) neutral ground state of Ti it has been suggested that one should allow mixing of the $3d^2 4p^2$ configuration with the $3d^2 4s^2$ configuration in the trial wave function because the $4p$ level is nearly degenerate with the $4s$ level.[29] We have performed variational quantum Monte Carlo (VMC) calculations for a number of different values of the mixing coefficient for the $3d^2 4p^2$ configuration, and have found that for each pseudopotential the optimum mixing coefficient is between 0.05 and 0.1. These mixing coefficients are considerably smaller than the values of 0.2–0.3 found by Mitas.[29] We have found that when the variational freedom of the Jastrow factor is restricted the optimal mixing coefficient increases and we believe that our smaller mixing coefficients are due to the greater variational flexibility of our Jastrow factor. The reduction in the energy of the $3d^2 4s^2$ neutral ground state obtained from the multideterminant trial wave function for the (^3F) neutral ground state is between 0.25 and 0.5 eV in VMC calculations, but in DMC calculations it is less than the statistical error bars given in Tables IV, V, VI, and VII, below.

V. RESULTS

A list of acronyms for the pseudopotentials we have tested is given in Table III. Our aim is to construct pseudopotentials for Si and Ti which work well in environments similar to the neutral atomic ground states. To quantify the accuracy of the pseudopotentials under these conditions we define the average error Δ,

$$\Delta = \sqrt{\sum_i \left(\frac{E_i^{\mathrm{DMC}} - E_i^{\mathrm{expt}}}{E_i^{\mathrm{expt}}} \right)^2}, \tag{18}$$

where E_i^{DMC} and E_i^{expt} are the DMC and experimental values for the energy differences from the neutral ground state obtained from the data in Tables IV and V for Si and Tables VI and VII for Ti. This measure of the error emphasizes the states close in energy to the neutral ground state. Other measures of the accuracy can be constructed from the data, but the trends are generally similar.

For Si, all the pseudopotentials tested perform at least reasonably well. The HW HF pseudopotential is significantly poorer than the others, and it performs worse that the HF pseudopotential we have generated. The effects of the CPP are small in Si, but it does improve the results for both the HF and semi-empirical (SE) pseudopotentials. The core re-

TABLE IV. Ionization energies of Si in eV calculated within DMC and compared with experimental values.

	First IP $3s^2 3p^2(^3P) \rightarrow 3s^2 3p^1(^2P)$	Second IP $3s^2 3p^1(^2P) \rightarrow 3s^2(^1S)$	Third IP $3s^2(^1S) \rightarrow 3s^1(^2S)$	Fourth IP $3s^1(^2S) \rightarrow 0$
Expt.	8.16	16.32	33.49	45.14
HW	8.339(14)	16.516(10)	33.137(6)	44.432(0)
HF	8.166(14)	16.278(17)	33.179(15)	44.553(0)
HF+CPP	8.168(12)	16.297(10)	33.448(6)	45.085(0)
LSDA	8.299(13)	16.583(18)	33.519(16)	45.080(0)
SE	8.137(16)	16.358(19)	33.552(15)	45.141(0)
SE+$V_{\mathrm{CPP}}^{e\text{-}e}$	8.067(16)	16.253(20)	33.394(19)	45.140(0)
SE-relax+$V_{\mathrm{CPP}}^{e\text{-}e}$	8.148(12)	16.259(13)	33.501(10)	45.197(0)

TABLE V. Excitation energies of Si in eV calculated within DMC and compared with experimental values.

	$3s^1 3p^1(^3P) \rightarrow 3s^1 3p^1(^1P)$	$3s^2 3p^2(^3P) \rightarrow 3s^1 3p^3(^5S)$	$3s^2 3p^1(^2P) \rightarrow 3s^1 3p^2(^4P)$	$3s^2(^1S) \rightarrow 3s^1 3p^1(^3P)$
Expt.	3.72	4.11	5.30	6.56
HW	4.079(10)	3.562(12)	4.731(9)	6.016(7)
HF	4.021(9)	3.909(13)	5.096(9)	6.363(15)
HF+CPP	3.810(9)	4.052(10)	5.264(9)	6.571(6)
LSDA	4.041(9)	3.827(10)	4.994(10)	6.232(16)
SE	4.022(9)	4.029(13)	5.223(12)	6.478(15)
SE+$V_{\mathrm{CPP}}^{e\text{-}e}$	3.774(9)	4.084(14)	5.282(10)	6.521(19)
SE-relax+$V_{\mathrm{CPP}}^{e\text{-}e}$	3.807(9)	4.077(10)	5.249(9)	6.561(10)

laxation corrections (see Table II) are also small, but they also improve the performance of our SE pseudopotential. The best performance of any of the pseudopotentials is given by our SE pseudopotential with core relaxation corrections and the full CPP including the two-electron term.

For Ti our HF pseudopotential gives the best results in our correlated calculations. We have also tested our HF pseudopotential within HF theory, where it performs very well. The most significant error in this case is the overestimation of the $s \rightarrow d$ promotion energy, which has been noted before in HF pseudopotentials.[30,31] This error arises because the $3d$ orbital is large near the outer node of the all-electron $4s$ orbital. The nodeless pseudo-$4s$ orbital is very different from the all-electron $4s$ orbital in this region and therefore an error is introduced into the Hartree and exchange interactions between the two orbitals. In the reference configuration this error is compensated by the pseudopotential, which by construction gives the correct energy eigenvalues, but in other configurations this compensation is incomplete and an error is introduced. In Ti the effect is to increase the energy of $s^1 d^3$ states. We have noticed a similar effect in a LSDA Ti pseudopotential created with a full nonlinear core exchange-correlation correction.[32] This demonstrates that the effect is generic and not dependent on the detailed description of exchange and correlation effects. It is therefore interesting that our DMC calculations for Ti with a HF pseudopotential do not show such an effect for the $3d^2 4s^2(^3F) \rightarrow 3d^3 4s^1(^5F)$ transition, for which we do not have an explanation.

The addition of the Shirley-Martin[12] CPP to our HF Ti pseudopotential reduces the accuracy obtained. Core-polarization effects are large for Ti because the core is highly polarizable and the energy of a Ti atom with one valence $3d$ electron is lowered by 1.45 eV on adding the CPP from Table 1(b) of Ref. 12. The resulting ionization energy is 2.99 eV larger than the experimental value, which suggests that the Shirley-Martin CPP for Ti is too attractive in the d channel. This observation largely explains the fairly poor results obtained in Tables VI and VII for the HF+CPP pseudopotential.

The Hay-Wade small core (HWS) Ti pseudopotential gives the next best results. It is interesting that the HWS pseudopotential, in which the $3s$ and $3p$ electrons are included in the valence, performs less well than our HF pseudopotential for states close in energy to the ground state. The small-core Ti neutral pseudoatom has 12 valence electrons while the large-core one has 4, and the computational cost of performing a DMC calculation using the small-core Ti pseudopotential is about an order of magnitude greater than using the large-core one. Note that the HWS pseudopotential performs quite well for highly ionized configurations, presumably because it is able to describe the relaxation of the $3s$ and $3p$ shells, which is not possible in the large-core pseudopotentials.

The next most accurate results were obtained with the DF Ti pseudopotential. This pseudopotential includes the most important relativistic effects and might be expected to give better results than our HF pseudopotential. The DF pseudo-

TABLE VI. Ionization energies of Ti in eV calculated within DMC and compared with experimental values.

	First IP $3d^2 4s^2(^3F) \rightarrow 3d^2 4s^1(^4F)$	Second IP $3d^2 4s^1(^4F) \rightarrow 3d^2(^3F)$	Third IP $3d^2(^3F) \rightarrow 3d^1(^2D)$	Fourth IP $3d^1(^2D) \rightarrow 0$
Expt.	6.82	13.58	27.49	43.24
HWL	6.544(12)	12.992(8)	27.942(4)	45.917(0)
HWS	6.590(38)	13.386(29)	27.295(38)	43.112(87)
DF	6.759(12)	13.354(7)	27.194(3)	44.113(0)
LSDA	6.799(11)	13.447(7)	26.574(4)	44.336(0)
HF	6.667(14)	13.223(6)	27.247(3)	44.774(0)
HF+CPP	6.724(12)	13.658(6)	28.407(2)	46.228(0)
SE	7.250(12)	14.064(8)	26.307(5)	43.236(0)
SE+$V_{\mathrm{CPP}}^{e\text{-}e}$	7.037(12)	13.997(6)	26.090(2)	43.236(0)
SE-relax+$V_{\mathrm{CPP}}^{e\text{-}e}$	7.119(12)	14.266(4)	27.326(2)	45.022(0)

TABLE VII. Excitation energies of Ti in eV calculated within DMC and compared with experimental values.

	$3d^2 4s^2(^3F) \rightarrow 3d^3 4s^1(^5F)$	$3d^2 4s^2(^3F) \rightarrow 3d^3 4p^1(^5G)$	$3d^2 4s^1(^4F) \rightarrow 3d^3(^4F)$	$3d^2(^3F) \rightarrow 3d^1 4s^1(^3D)$	$3d^1 4s^1(^3D) \rightarrow 3d^1 4s^1(^1D)$
Expt.	0.81	3.29	0.11	4.72	0.42
HWL	0.320(14)	4.155(29)	−0.337(10)	6.108(5)	0.415(6)
HWS	0.678(52)	3.078(54)	0.173(47)	4.457(24)	0.488(24)
DF	1.089(13)	3.770(20)	0.537(8)	4.714(4)	0.377(4)
LSDA	1.525(15)	4.118(15)	1.051(10)	4.054(4)	0.125(5)
HF	0.837(16)	3.324(17)	0.181(9)	5.067(4)	0.090(7)
HF+CPP	0.472(14)	3.123(16)	−0.107(8)	5.490(3)	0.509(5)
SE	1.427(16)	4.403(17)	1.154(10)	3.280(5)	0.052(4)
SE+$V_{\mathrm{CPP}}^{e\text{-}e}$	1.551(13)	4.465(16)	1.306(8)	3.151(3)	0.383(5)
SE-relax+$V_{\mathrm{CPP}}^{e\text{-}e}$	1.389(14)	4.308(14)	1.084(6)	3.831(3)	0.439(5)

potential of Hurley *et al.*[23] was created using a different scheme from our pseudopotentials and has a very different functional form, and therefore detailed comparisons of results may not be valid. Relativistic effects for the valence electrons in Ti are in fact fairly small, the major effects being to raise the *d* level and lower the *s* level slightly. Our HF pseudopotentials do not contain relativistic effects although when we add a CPP we are including relativistic effects because they are implicit in the CPP parameters given in Table 1(b) of Ref. 12. Our SE pseudopotentials contain relativistic effects through the use of experimental energies. Our LSDA pseudopotentials for both Si and Ti also contain relativistic effects, although in both cases their performance in correlated calculations is inferior to the HF pseudopotentials.

Mitas[29] has published VMC and DMC results for a Ti pseudoatom using the large-core pseudopotential of Pacios and Olcina,[31] which is a Dirac-Fock pseudopotential which was designed to reproduce energy differences. Mitas[29] reported six energy differences, of which four are directly comparable with our results. For these four energy differences our HF pseudopotential performs a little better.

Our Ti SE pseudopotential does not perform very well. The introduction of the two-electron CPP term actually makes the results even worse, while the core-relaxation effects give a small improvement. The core-relaxation effects are large in Ti, especially for the *d* level, which is shifted downwards in energy to 1.79 eV, although we believe that our corrections for core relaxation are soundly based and should account for the majority of these effects. We remarked above that we believe that the Shirley-Martin CPP for Ti is too attractive in the *d* channel and this introduces errors into our SE+$V_{\mathrm{CPP}}^{e\text{-}e}$ pseudopotential via the two-electron CPP term. To explore the lack of success of the SE pseudopotential for Ti in more detail we have performed Hartree-Fock calculations for the different pseudopotentials. These show that in the neutral ground state the *s* level of our SE Ti pseudopotential is 0.47 eV lower than for the HF pseudopotential, while the *d* level is 1.42 eV higher than for the HF pseudopotential. The consequences of these differences can clearly be seen in the results of Tables VI and VII. For example, the first IP of the SE pseudopotential, which corresponds to the removal of an *s* electron, is 0.571 eV larger than the HF pseudopotential value, and the $s \rightarrow d$ promotion energy is 0.578 eV larger than the HF pseudopotential value.

In the single-valent ion the *s* level of our HF pseudopotential is 0.76 eV above the experimental ionization energy, and the effect of core relaxation on going from the neutral to ionized core is to raise it by a further 0.80 eV. Core-relaxation effects are therefore not the source of the differences between the HF and SE pseudopotentials. Also core polarization, even when estimated using the Shirley-Martin CPP which we believe overestimates these effects, is too small to explain the differences. The picture that emerges is that the relative failure of our SE pseudopotentials for Ti is *not* due to core-relaxation effects or core-polarization effects, but is due to errors in describing the interactions between the *s* and *d* valence electrons. The HF pseudopotential generated in the neutral configuration includes corrections for the difference between the all-electron and pseudovalence orbitals, but our SE pseudopotential does not.

This effect has been discussed before in the context of HF calculations.[30,31] Attempts have been made to alter the *s* pseudopotential to force the pseudo-orbital to look more like the all-electron 4*s* orbital, although the success of this approach has been limited.[30] It would appear, however, that some method of correcting the interactions between the pseudo-orbitals is necessary to achieve higher accuracy in HF and correlated calculations of Ti. We could of course alter the eigenvalues of the SE pseudopotentials to improve their accuracy for near-neutral configurations. However, this would run counter to the spirit of our approach, in which we try and construct the SE pseudopotential using a clearly defined strategy rather than just fitting to the energy differences, and it would still not solve the problem of the interactions between the pseudo-orbitals.

VI. CONCLUSIONS

We have introduced a method for generating semiempirical pseudopotentials for use in correlated wave-function calculations. Our semiempirical pseudopotentials are generated in single-valent atomic configurations, but we have developed a scheme which enables us to apply core-relaxation corrections so that the pseudopotential works better in near-

neutral configurations. For Si the semiempirical pseudopotential is the most accurate that we have been able to generate, giving errors of only a few hundredths of an eV for a wide range of states. This high level of transferability within correlated calculations is similar to the transferability obtained in density-functional theory pseudopotential calculations (provided nonlinear core-exchange-correlation corrections are included[32]) and Hartree-Fock pseudopotential calculations for Si. We believe that our semiempirical scheme should work very well for all atoms up to at least atomic number 18 and is probably the most accurate currently available scheme for generating pseudopotentials for correlated wave-function calculations for these atoms.

Our semiempirical scheme has not proved successful for Ti and the best results we have obtained for this atom are with a Hartree-Fock pseudopotential. The main reason for the relative failure of our SE pseudopotential for Ti is that it does not account for the differences in the interactions between the all-electron orbitals and pseudo-orbitals.

In Si and Ti, at least, Hartree-Fock pseudopotentials give better results in correlated calculations than local-spin-density-approximation pseudopotentials. The core-polarization potential of Shirley and Martin[12] works well in Si, but not in Ti where it overestimates the core-polarization energy. Core-polarization effects are significant in transition metal elements and it is important to develop accurate core-polarization potentials for these elements.

ACKNOWLEDGMENTS

We thank Eric Shirley for useful discussions. Financial support was provided by the Engineering and Physical Sciences Research Council (UK). Computational resources on a COMPAQ multiprocessor (Columbus cluster), provided by the U.K. Computational Chemistry Facility at the Rutherford Appleton Laboratory (Department of Chemistry, King's College London, Strand, London WC2R 2LS), are acknowledged. Many of the DMC calculations were performed on the Hitachi SR2201 located at the University of Cambridge High Performance Computing Facility.

*Present address: National Renewable Energy Laboratory, Golden, CO 80401.

[1] D. Ceperley, G. Chester, and M. Kalos, Phys. Rev. B **16**, 3081 (1971).
[2] B. L. Hammond, W. A. Lester, and P. J. Reynolds, *Monte Carlo Methods in Ab Initio Quantum Chemistry* (World Scientific, Singapore, 1994).
[3] D. M. Ceperley, J. Stat. Phys. **43**, 815 (1986).
[4] P. A. Christiansen, Y. S. Lee, and K. S. Pitzer, J. Chem. Phys. **71**, 4445 (1979).
[5] D. R. Hamann, M. Schlüter, and C. Chiang, Phys. Rev. Lett. **43**, 1494 (1979).
[6] G. B. Bachelet, D. R. Hamann, and M. Schlüter, Phys. Rev. B **26**, 4199 (1982).
[7] W. Müller, J. Flesch, and W. Meyer, J. Chem. Phys. **80**, 3297 (1984).
[8] V. Heine and I. V. Abarenkov, Philos. Mag. **9**, 451 (1964).
[9] I. V. Abarenkov and V. Heine, Philos. Mag. **12**, 529 (1965).
[10] P. H. Acioli and D. M. Ceperley, J. Chem. Phys. **100**, 8169 (1994).
[11] J. Callaway, Phys. Rev. **106**, 868 (1957).
[12] E. L. Shirley and R. M. Martin, Phys. Rev. B **47**, 15 413 (1993).
[13] S. Bashkin and J. O. Stoner, Jr., *Atomic Energy Levels and Grotrian Diagrams* (North-Holland, Amsterdam, 1975), Vol. 1.
[14] C. Fröse Fischer, Comput. Phys. Commun. **43**, 355 (1987).
[15] M. J. Frisch *et al.*, *GAUSSIAN 94 User's Manual* (Gaussian Inc., Pittsburgh, PA, 1995).
[16] G. Arfken, *Mathematical Methods for Physicists* (Academic Press, Orlando, FL, 1985).
[17] N. Troullier and J. L. Martins, Phys. Rev. B **43**, 1993 (1991).
[18] C. W. Greeff and W. A. Lester, Jr., J. Chem. Phys. **109**, 1607 (1998).
[19] M. Krauss and W. J. Stevens, Annu. Rev. Phys. Chem. **35**, 357 (1984).
[20] P. J. Hay and W. R. Wadt, J. Chem. Phys. **82**, 284 (1985).
[21] P. J. Hay and W. R. Wadt, J. Chem. Phys. **82**, 270 (1985).
[22] P. J. Hay and W. R. Wadt, J. Chem. Phys. **82**, 299 (1985).
[23] M. M. Hurley, L. F. Pacios, P. A. Christiansen, R. B. Ross, and W. C. Ermler, J. Chem. Phys. **84**, 6840 (1986).
[24] T. Kato, Commun. Pure Appl. Math. **10**, 151 (1957).
[25] C. J. Umrigar, K. G. Wilson, and J. W. Wilkins, Phys. Rev. Lett. **60**, 1719 (1988).
[26] P. R. C. Kent, R. J. Needs, and G. Rajagopal, Phys. Rev. B **59**, 12 344 (1999).
[27] M. M. Hurley and P. A. Christiansen, J. Chem. Phys. **86**, 1069 (1987); B. L. Hammond, P. J. Reynolds, and W. A. Lester, Jr., *ibid.* **87**, 1130 (1987); L. Mitas, E. L. Shirley, and D. M. Ceperley, *ibid.* **95**, 3467 (1991).
[28] W. M. C. Foulkes, R. Q. Hood, and R. J. Needs, Phys. Rev. B **60**, 4558 (1999).
[29] L. Mitas, in *Computer Simulation Studies in Condensed Matter Physics V*, edited by D. P. Landau, K. K. Mon, and H. B. Schüttler (Springer, Berlin, 1993).
[30] E. C. Walker, P. A. Christiansen, and L. F. Pacios, Mol. Phys. **63**, 139 (1988).
[31] L. F. Pacios and V. B. Olcina, J. Chem. Phys. **95**, 441 (1991).
[32] S. G. Louie, S. Froyen, and M. L. Cohen, Phys. Rev. B **26**, 1738 (1982).